doi:10.1093/brain/awv397 BRAIN 2016: 139; 738–750 | 738

BRAIN
A JOURNAL OF NEUROLOGY

Non-invasive imaging of oxygen extraction fraction in adults with sickle cell anaemia

Lori C. Jordan,[1] Melissa C. Gindville,[1] Allison O. Scott,[2] Meher R. Juttukonda,[2] Megan K. Strother,[2] Adetola A. Kassim,[3] Sheau-Chiann Chen,[4] Hanzhang Lu,[5] Sumit Pruthi,[2] Yu Shyr[4] and Manus J. Donahue[2,6,7]

Sickle cell anaemia is a monogenetic disorder with a high incidence of stroke. While stroke screening procedures exist for children with sickle cell anaemia, no accepted screening procedures exist for assessing stroke risk in adults. The purpose of this study is to use novel magnetic resonance imaging methods to evaluate physiological relationships between oxygen extraction fraction, cerebral blood flow, and clinical markers of cerebrovascular impairment in adults with sickle cell anaemia. The specific goal is to determine to what extent elevated oxygen extraction fraction may be uniquely present in patients with higher levels of clinical impairment and therefore may represent a candidate biomarker of stroke risk. Neurological evaluation, structural imaging, and the non-invasive T_2-relaxation-under-spin-tagging magnetic resonance imaging method were applied in sickle cell anaemia ($n = 34$) and healthy race-matched control ($n = 11$) volunteers without sickle cell trait to assess whole-brain oxygen extraction fraction, cerebral blood flow, degree of vasculopathy, severity of anaemia, and presence of prior infarct; findings were interpreted in the context of physiological models. Cerebral blood flow and oxygen extraction fraction were elevated ($P < 0.05$) in participants with sickle cell anaemia ($n = 27$) not receiving monthly blood transfusions (interquartile range cerebral blood flow = 46.2–56.8 ml/100 g/min; oxygen extraction fraction = 0.39–0.50) relative to controls (interquartile range cerebral blood flow = 40.8–46.3 ml/100 g/min; oxygen extraction fraction = 0.33–0.38). Oxygen extraction fraction ($P < 0.0001$) but not cerebral blood flow was increased in participants with higher levels of clinical impairment. These data provide support for T_2-relaxation-under-spin-tagging being able to quickly and non-invasively detect elevated oxygen extraction fraction in individuals with sickle cell anaemia with higher levels of clinical impairment. Our results support the premise that magnetic resonance imaging-based assessment of elevated oxygen extraction fraction might be a viable screening tool for evaluating stroke risk in adults with sickle cell anaemia.

1 Department of Pediatrics, Division of Pediatric Neurology, Vanderbilt University Medical Center, Nashville, TN, USA
2 Department of Radiology and Radiological Sciences, Vanderbilt University Medical Center, Nashville, TN, USA
3 Vanderbilt-Meharry Center of Excellence in Sickle Cell Disease, Vanderbilt University Medical Center, Nashville, TN, USA
4 Center for Quantitative Sciences, Vanderbilt University Medical Center, Nashville, TN, USA
5 Russell H. Morgan Department of Radiology and Radiological Science, The Johns Hopkins University School of Medicine, Baltimore, MD, USA
6 Department of Psychiatry, Vanderbilt University Medical Center, Nashville, TN, USA
7 Department of Neurology, Vanderbilt University Medical Center, Nashville, TN, USA

Correspondence to: Lori C. Jordan, MD, PhD
Department of Pediatrics,
Division of Pediatric Neurology,
Vanderbilt University Medical Center,
Nashville, TN 37232
E-mail: lori.jordan@vanderbilt.edu

Keywords: arterial spin labelling; brain ischaemia; cerebral haemodynamics; oxygen extraction fraction; sickle cell anaemia

Received August 28, 2015. Revised November 12, 2015. Accepted November 30, 2015. Advance Access publication January 27, 2016

Abbreviations: CBF/V = cerebral blood flow/volume; $CMRO_2$ = cerebral metabolic rate of oxygen consumption; OEF = oxygen extraction fraction; SCA = sickle cell anaemia; TRUST = T_2-relaxation-under-spin-tagging

Introduction

Sickle cell anaemia (SCA) is a well-characterized monogenetic disorder with a high prevalence of cerebral vasculopathy, silent cerebral infarcts, and overt stroke (Debaun *et al.*, 2006). Among children with SCA the incidence of stroke is 2–3/1000/year and in adults with SCA the incidence is even higher at ~5–13/1000/year (Ohene-Frempong *et al.*, 1998). In these patients, strokes are the most frequent cause of long-term disability, and consist of ~75% ischaemic strokes and 25% haemorrhagic strokes (Adams *et al.*, 1998*a*), with an overall lifetime prevalence of overt or silent cerebral infarcts estimated at 30–50% (Ohene-Frempong *et al.*, 1998). Primary stroke prevention in children 2 to 16 years of age with SCA includes transcranial Doppler ultrasound cerebral artery velocity assessment annually and for those that have an elevated measurement, regular, monthly blood transfusion therapy for at least 1 year followed by indefinite treatment with oral hydroxyurea (National Heart, 2014). Transfusions result in ~90% relative risk reduction in overt strokes (Adams *et al.*, 1998*b*).

However, no accepted screening measure exists for identifying adults with SCA at high risk for strokes. Despite the high clinical utility of transcranial Doppler ultrasound measurement for identifying children with SCA at increased risk for future strokes, this method has not been validated for stroke risk assessment in adults with SCA. In one study, adults showed lower velocities than children despite continued stroke risk (Valadi *et al.*, 2006). Given the high rate of adults with ischaemic strokes, coupled with the improved survival of children with SCA to adulthood, the field urgently needs an imaging strategy that will identify adults that have an increased risk of ischaemic stroke to allow targeted primary stroke prevention strategies. The critical barrier to addressing this issue rests with a general inability to identify underlying brain tissue-level impairment that may provide evidence-based biomarkers for therapy.

Screening procedures generally focus on quantifying hemodynamic and metabolic changes that may be most prognostic for new or recurrent stroke. Physiologically, risk for ischaemic stroke occurs when cerebral blood flow (CBF; ml blood/100 g tissue/min) and cerebral blood volume (CBV; ml blood / ml parenchyma) are inadequate to maintain the cerebral metabolic rate of oxygen consumption ($CMRO_2$; μmol O_2/100 g tissue/min). $CMRO_2$ is the product of CBF, the oxygen extraction fraction from blood (OEF; ratio of oxygen to oxygen delivered) and blood oxygen content. The blood oxygen content is generally decreased in patients with SCA owing to reduced haematocrit, the presence of haemoglobin SS (HbSS) and reduced haemoglobin-bound oxygen.

CBV may increase with cerebral autoregulatory vasodilation, however, this response is variable in the setting of steno-occlusion (Derdeyn *et al.*, 2002), and in anaemia, contrary to vasodilation in proximal larger arterioles, small pial arterioles (<100-μm diameter) may constrict in a manner that depends on haematocrit (Hudak *et al.*, 1989). Typically, in humans and animals exposed to anaemia or haemodilution, CBF increases when haemoglobin levels decrease (Vorstrup *et al.*, 1992; Prohovnik *et al.*, 2009). However, for intermediate-to-significant reductions in cerebral perfusion pressure and arterial steno-occlusion, as is common in advanced moyamoya that occurs in SCA, the extent of autoregulatory capacity may dictate the magnitude and direction of CBF and CBV changes (Fig. 1) (Powers, 1991; Derdeyn *et al.*, 2002). Therefore, there may be a wide variation of changes in CBF and CBV in SCA, and these variations depend on severity of anaemia and vasculopathy extent. As such, CBF and CBV are incomplete indicators of disease severity.

In the presence of reduced oxygen delivery secondary to anaemia or flow-limiting stenosis, OEF should increase in the presence of unchanging $CMRO_2$. Therefore, in steno-occlusive disease, OEF has been postulated to be a more sensitive indicator of critical tissue-level impairment for cerebral ischaemia and eventual strokes, compared to CBF or CBV, over a larger range of haemodynamic impairment (Derdeyn *et al.*, 1999, 2001). However, neuroimaging methods for evaluating OEF routinely in the clinic have remained elusive and more limited information is available on the role of OEF for predicting clinical impairment in the setting of reduced oxygen delivery in SCA.

OEF can be assessed by methods such as $_{15}O$ PET, and PET data have greatly increased our understanding of flow-metabolism relationships (Fox and Raichle, 1986; Derdeyn *et al.*, 2002). A large range of OEF was also observed in a $_{15}O$ PET study in a small group of heterogeneous patients with SCA ($n = 6$; OEF = 0.37–0.52) (Herold *et al.*, 1986); however, the mean OEF was only slightly and not significantly elevated (OEF = 0.44 ± 0.07) relative to control OEF (OEF = 0.42 ± 0.04). OEF-PET studies in a larger number of participants have not been conducted to our knowledge, partly owing to the fact that $_{15}O$ PET is only available in specialized centres with on-site cyclotrons and requires ionizing radiation as well as arterial blood sampling. Limited widespread availability of methodologies for measuring OEF has prevented hypotheses regarding OEF,

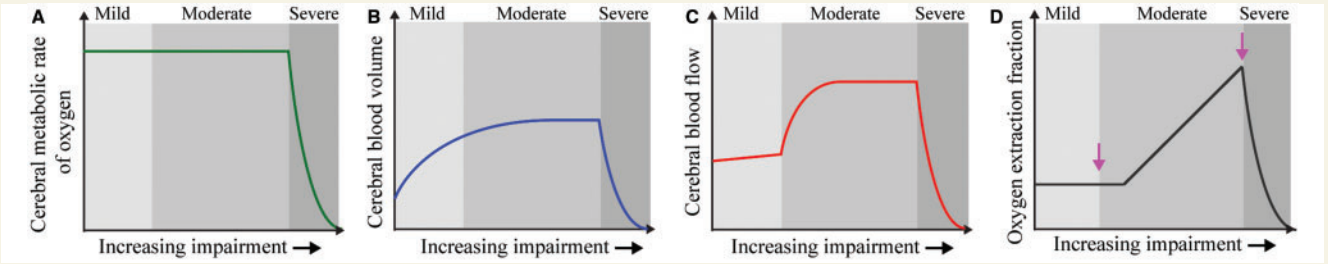

Figure 1 Mechanistic model for increasing stages of haemo-metabolic impairment in SCA. (**A**) Cerebral metabolic rate of oxygen consumption remains constant until severe impairment. (**B**) Large arteriole CBV may increase on average in moderate stages via vasodilation to maintain CBF. (**C**) CBF increases sharply in moderate stages to maintain adequate delivery of oxygen to tissue. (**D**) Once autoregulatory capacity is reached, or vasculopathy becomes severe, CBF plateaus or declines and OEF increases. When oxygen can no longer be supplied by these mechanisms, a stroke occurs. We postulate that in adults with SCA, elevated oxygen extraction fraction (**D**) can be used to identify those at increased risk of having new ischaemic events.

vasculopathy, and therapy response from being rigorously evaluated in adults with SCA.

Alternatively, whole-brain OEF can be assessed quickly and non-invasively using MRI. Specifically, the blood water transverse relaxation time (T_2) depends very sensitively on oxygenation level and haematocrit, and therefore combined measurements of haematocrit and venous T_2 can be converted to blood oxygenation level through appropriate blood signal isolation and calibration procedures. Elegant work has demonstrated the dependence between venous T_2 and blood oxygenation level (Zhao *et al.*, 2007; Lu *et al.*, 2012), and T_2-relaxation-under-spin-tagging (TRUST) has recently been developed and compared to pulse oximetry in healthy adults, and has been shown to provide similar arterial cerebral blood oxygen levels for normoxic and hypoxic conditions as pulse oximetry (Lu *et al.*, 2012). TRUST has been used to quantify OEF in healthy adults across the lifespan (Lu *et al.*, 2011) and has also been applied in conjunction with measurements of excitation/inhibition balance in healthy tissue (Rane *et al.*, 2015), in patients with autoimmune disorders (Ge *et al.*, 2012), and in neonates (Liu *et al.*, 2014). While TRUST can be applied quickly (1–2 min) with minimal user expertise, making it an appealing clinical tool, a limitation is that it only provides a whole-brain assessment of OEF, and as such is most suitable for conditions with global pathophysiological alterations.

SCA represents a potentially ideal application for TRUST, as global elevation in OEF secondary to anaemia may be a significant stroke risk factor (Hulbert and Ford, 2014), rather than focal regions of impairment downstream from stenotic vessels as only ~15% of adults with SCA have intracranial stenosis (Silva *et al.*, 2009) and many without stenosis have infarcts (Hulbert and Ford, 2014). Therefore, the purpose of this study was to apply TRUST in sequence with more conventional measures of disease in a controlled cohort of participants with SCA without significant vasculopathy or extensive neurological impairment.

The primary hypothesis is that in a relatively homogenous cohort of adult participants with SCA with similar medical management (e.g. hydroxyurea), neurological function, and without significant vasculopathy, whole brain OEF is elevated compared to age and race-matched controls with normal haemoglobin genotype. A secondary hypothesis is that in a broader cohort of adults with SCA with more varied history and treatment regimen (e.g. hydroxyurea or blood transfusion), OEF is highest in participants with the highest levels of clinical impairment as defined by vasculopathy extent, prior overt stroke, and/or chronic SCA-related pain. A long-term goal for this sort of methodology is to assess whether metabolic neuroimaging can predict overt stroke in adults with SCA, and if so to use this method as a screening test for stroke risk in adults with SCA for whom no accepted test is currently available.

Materials and methods

Participant demographics

All volunteers ($n = 45$) provided informed, written consent in accordance with the ethical standards and approval of the Vanderbilt University Institutional Review Board. Participants with SCA (ages 18–40 years; defined as genotype haemoglobin SS and S-Beta^0 thalassemia) were recruited from a comprehensive sickle cell disease clinic.

The total volunteer cohort comprised three distinct populations for different sub-studies: (i) healthy controls; (ii) SCA volunteers receiving hydroxyurea or no disease-modifying therapy; and (iii) SCA volunteers receiving blood transfusion.

Healthy controls ($n = 11$; age = 26.9 ± 5.1 years; sex = 5/6 male/female) matched for gender, race and age with SCA participants and with no major health problems were recruited by advertisement.

Participants with SCA are seen in clinic every 1–6 months and were recruited during a routine clinic visit. As part of routine care, children and adults with sickle cell anaemia may be treated with hydroxyurea to reduce the number of painful vaso-occlusive crises and ameliorate disease expression. They also may receive regular blood transfusions (approximately monthly) for primary or secondary stroke prevention, or to ameliorate severe disease expression such as severe, recurrent pain episodes. To study a relatively homogenous

patient population for purposes of testing the primary hypothesis, participants with SCA ($n = 27$; age = 27.7 ± 5.0 years; sex = 16/11 male/female) did not receive blood transfusion and had no moderate stenosis >50% of any major intracranial or extracranial vessel. To evaluate the secondary hypothesis, additional participants with SCA ($n = 7$; age = 31.5 ± 4.3 years; sex = 2/5 male/female) were recruited with prior stroke and/or chronic debilitating pain requiring blood transfusions and all SCA participants ($n = 34$) were divided as to those with less clinical impairment ($n = 15$; age = 25.9 ± 4.8 years; sex = 10/5 male/female) or more clinical impairment ($n = 19$; age = 30.5 ± 4.5 years; sex = 8/11 male/female). Clinical impairment was defined as moderate vasculopathy >50% of any major extracranial or intracranial vessel, prior overt stroke or infarct on neuroimaging, and/or chronic debilitating SCA-related pain that required treatment with chronic blood transfusion therapy. Seven of these patients were receiving blood transfusions and they were scanned late in their transfusion cycle (27.7 ± 11.4 days), when their haematocrit was near nadir. Patients on blood transfusions were evaluated separately to understand whether there were any significant differences in CBF and OEF in patients with more severe disease compared to the more homogenous sample of patients treated only with hydroxyurea.

Laboratory and neurological evaluations

Cases and controls had haematocrit measured within 7 days of imaging. Cases had known genotype haemoglobin SS or haemoglobin S-Beta^0 thalassemia, confirmed by haemoglobin evaluation (high performance liquid chromatography) as part of clinical care. Controls also had haemoglobin evaluation as part of the study to confirm that their genotype was normal adult haemoglobin AA with no evidence of sickle cell trait.

All participants had a standardized neurological examination by a board-certified neurologist that assessed mental status, cranial nerves, motor and sensory function, tendon reflexes, cerebellar function and gait, and the modified Rankin scale (Banks and Marotta, 2007) was scored.

Imaging

MRI and angiography were performed at 3 T (Philips) using body coil transmission and an array head coil for reception. Physiological monitoring (In Vivo Research Inc) included arterial oxygenation saturation via pulse oximetry, heart rate, and blood pressure.

Standard non-contrast structural head and neck magnetic resonance angiography was performed using the following sequences. T_1-weighted imaging: magnetization-prepared rapid gradient echo (MP-RAGE); spatial resolution = 1.0 × 1.0 × 1.0 mm^3; 3D turbo-field-echo; repetition time/echo time = 8.2/3.7 ms; T_2-weighted imaging: spatial resolution = 0.6 × 0.6 × 4.0 mm^3; turbo spin echo; repetition time/echo time = 3000/80 ms; T_2-weighted axial fluid attenuated inversion recovery imaging: spatial resolution = 0.9 × 1.1 × 3.0 mm^3; turbo inversion recovery; repetition time/inversion time/echo time = 11 000/2800/120 ms; T_2-weighted coronal fluid attenuated inversion recovery imaging: spatial resolution = 0.9 × 1.1 × 3.0 mm^3; turbo inversion recovery; repetition time/inversion time/echo time = 11 000/2800/120 ms; intracranial time-of-flight magnetic resonance angiography: spatial resolution = 0.5 × 0.8 × 1.4 mm^3; 3D T_1-weighted gradient echo; repetition time/echo time = 23/3.5 ms; cervical time-of-flight magnetic resonance angiography: spatial resolution = 0.9 × 0.9 × 3.0 mm^3; 2D T_1-weighted gradient echo; repetition time/echo time = 18.6/3.2 ms.

Pseudo-continuous arterial spin labelling was applied for CBF quantitation: spatial resolution = 3 × 3 × 7 mm^3; multislice 2D single-shot echo planar imaging; repetition time/echo time = 3675/13 ms; averages = 20. For labelling, a 1000 ms pulse train was used, followed by a post-labelling delay of 1900 ms. Pseudo-continuous arterial spin labelling was chosen, as compared to pulsed arterial spin labelling, with long post-labelling delay with parameters consistent with recent recommendations from the International Society for Magnetic Resonance in Medicine perfusion study group (Alsop *et al.*, 2015), to desensitize the sequence to differences in bolus arrival time that may be present between controls and patients with higher flow velocities. These considerations are addressed in the 'Discussion' section. An equilibrium magnetization (M_0) image was acquired with identical readout parameters as the arterial spin labelling scan but with spin labelling turned off and repetition time = 20 s. Reproducibility of this arterial spin labelling variant and sensitivity of CBF to changes in bolus arrival times has been evaluated previously (Donahue *et al.*, 2014).

TRUST (Lu and Ge, 2008) was applied for whole-brain OEF quantification and was repeated once in each subject for repeatability assessment. A subgroup ($n = 6$) of controls also returned for a second imaging session (gap = 1–4 months) to evaluate OEF and assess inter-session reproducibility. The principle of TRUST is to quantify OEF by comparing the difference in oxygenation level of blood entering the brain through the arteries to blood leaving the brain through the superior sagittal sinus. Venous blood water signal in the superior sagittal sinus is isolated using principles of venous spin labelling, and a T_2-preparation module is used to allow for variable T_2-weighting and venous T_2 to be quantified. The venous T_2 is then related to venous blood oxygenation level using established models and measured haematocrit values (Lu *et al.*, 2012), and OEF is quantified by incorporating additional information of arterial blood oxygenation saturation from peripheral pulse oximetry.

TRUST (Fig. 2) consists of a presaturation pulse and dephasing gradient, followed by a spatially-selective inversion pulse placed 25 mm distal to a single imaging slice planned 20 mm above the foramen magnum. The venous water labelling occurs in alternating acquisitions (e.g. 'label' acquisition), which are interleaved with 'control' acquisitions in which the venous water is not labelled. A post-labelling delay time of 1022 ms is allowed, during which the labelled blood water flows into the imaging region. During this period, a non-selective T_2-preparation module is applied with varying duration (effective echo time). The T_2-preparation module consists of a non-selective $\pi/2$ pulse followed by a string of refocusing pulses with constant inter-pulse spacing (Car-Purcell-Meiboom-Gill sequence $-\tau = 10$ms), and concludes with a $-\pi/2$ pulse. The T_2 module was performed for effective echo times = 0, 40, 80, and 160 ms (four averages per effective echo time; repetition time = 1978 ms). Following the T_2-preparation, a single-shot gradient echo echo-planar-imaging

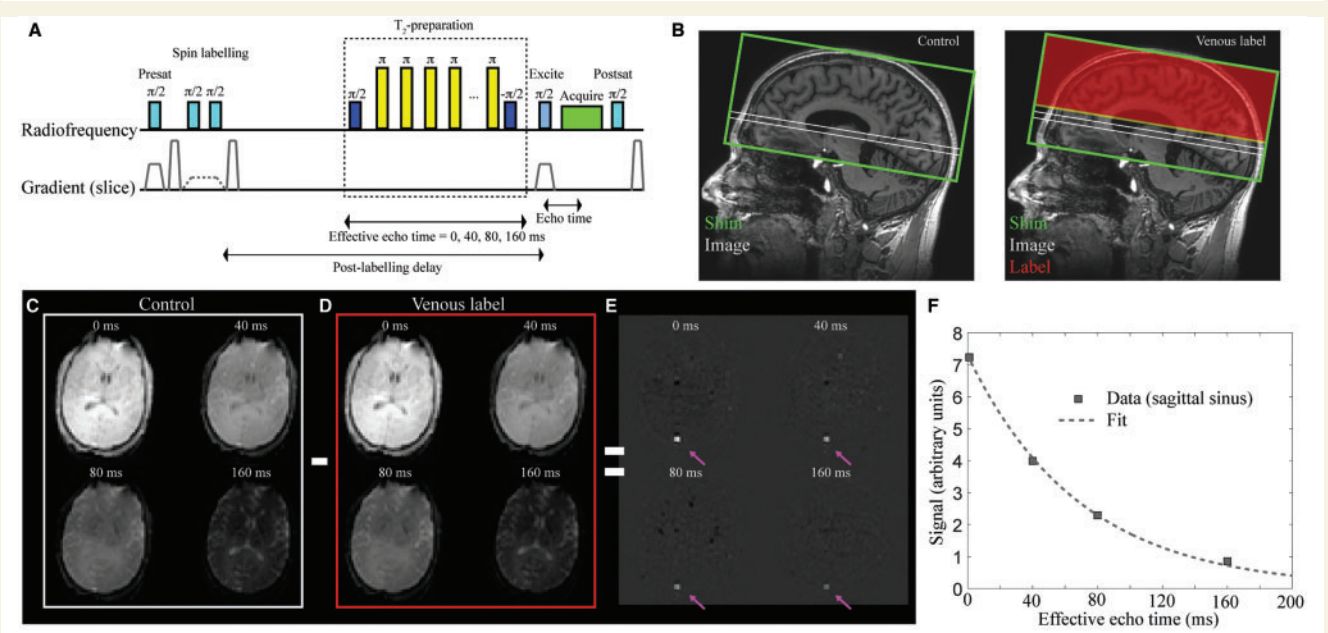

Figure 2 The TRUST MRI approach for quantifying whole-brain OEF. The pulse-sequence is shown in **A** and a conceptual representation of the method is shown in **B**. Briefly, the method consists of a presaturation pulse followed by an inversion pulse and corresponding gradient for labelling venous blood water in a label condition or inversion pulse with no gradient for a control condition. Following the venous blood water labelling (**B**; red), a post-labelling delay (PLD = 1022 ms) is prescribed during which a T_2-preparation module with varying duration (duration = effective echo time) allows for variable T_2-weighting. An image (**B**; white) is acquired at the level of the supratentorial sagittal sinus, ~20 mm above the foramen magnum. The difference in signal between control (**C**) and label (**D**) acquisitions yields only venous signal in the superior sagittal sinus (**E**), which allows for venous T_2 and corresponding oxygenation level to be determined upon application of appropriate models.

readout (parallel imaging factor = 3; partial *k*-space factor = 0.7; echo time = 3.6 ms) is applied, and the sequence ends with a post-saturation excitation pulse and dephasing gradient for spin reset. By varying the duration of the T_2-preparation, it is possible to generate T_2-weighting. The T_2-preparation module is used rather than a simple multi-echo time approach to reduce sensitivity to blood water outflow over the duration of the readout.

Structural imaging analysis

Cervical and major intracranial vessels for each participant were assessed for vasculopathy by a board-certified neuroradiologist as previously described (Hulbert *et al.*, 2011). Each vessel was graded as normal, mild stenosis (25–50%), moderate stenosis (51–69%), severe stenosis (70–99%), or occlusion. Severity of intracranial vasculopathy was graded by the worst vessel seen, as mild, moderate, severe, or occluded (Hulbert *et al.*, 2011).

Infarcts were classified by the same neuroradiologist. First, the scan was judged as normal or abnormal. If abnormal, the lesions were assigned as either (i) non-specific white matter lesion if <3 mm in diameter (Casella *et al.*, 2010) and visible in at least two planes of fluid-attenuated inversion recovery (FLAIR) images (axial and coronal) (Casella *et al.*, 2010); or (ii) focal, discrete ischaemic infarcts if >3 mm in two planes (Wardlaw *et al.*, 2013). The above criteria were also applied to control volunteer datasets to confirm the absence of flow-limiting vasculopathy and infarct.

Volumetric, CBF and OEF quantification procedures

To allow for tissue volumetric comparisons, the skull was extracted from anatomical T_1-weighted images and grey matter, white matter, and total CSF volume fractions were calculated (Jenkinson and Smith, 2001; Zhang *et al.*, 2001). Total tissue volumes and total tissue volumes normalized by intracranial volume were recorded.

Arterial spin labelling data were corrected for motion using standard affine routines (Jenkinson and Smith, 2001), surround-subtracted (Lu *et al.*, 2006), and averaged over all measurements to generate the mean difference magnetization. CBF was quantified in each voxel according to Alsop *et al.* (2015):

$$CBF = \frac{6000 \cdot \lambda \cdot \Delta M \cdot e^{PLD/T_{1,b}}}{2 \cdot \alpha \cdot T_{1,b} \cdot M_0 \cdot \left(1 - e^{-\tau/T_{1,b}}\right)} \quad (1)$$

where λ = 0.9 ml/g is the blood–brain partition coefficient, ΔM is the mean difference magnetization, PLD is the post-labelling delay = 1900 ms, $T_{1,b}$ is the blood water T_1, α = 0.80 is the pseudocontinuous arterial spin labelling efficiency, M_0 is the equilibrium magnetization (taken from the M_0 image), and τ = 1000 ms is the duration of the labelling pulse train. The factor 6000 is incorporated to convert the CBF units from ml/g/s to conventional ml/100 g/min. Importantly, $T_{1,b}$ will vary with haematocrit. While a single value for this parameter of ~1650 ms is commonly assumed in healthy

participants (Alsop *et al.*, 2015), $T_{1,b}$ will decrease with haematocrit, which will lead to a slower decay of the blood water label and an overestimation of CBF if not taken into account. Therefore, $T_{1,b}$ was quantified on an individual participant basis using measured haematocrit values and the known relationship between arterial blood T_1 and haematocrit (Hct) at 3 T (Lu *et al.*, 2004),

$$T_{1,b} = (0.52 \cdot Hct + 0.38)^{-1} \quad (2)$$

The relationship between haematocrit and $T_{1,b}$ has been characterized in blood of normal individuals with haemoglobin AA, however to ensure that the relationship between haematocrit, $T_{1,b}$, and blood with HbSS was not a primary contributing factor to our results, we performed *ex vivo* calculations of blood water relaxation times in blood from individuals with SCA that has predominantly haemoglobin S (see 'Discussion' section). CBF was quantified in the native space for each voxel, after which the data were transformed to the high spatial resolution native T_1 space and subsequently to a 2 mm T_1-weighted Montreal Neurological Institute atlas. CBF was recorded in grey matter, separately in right and left internal carotid artery flow territories, as well as the basilar flow territory using previously calculated masks derived from vessel-encoded arterial spin labelling data from 92 subjects (Fig. 3) (Faraco *et al.*, 2015). Grey matter was the focus of this analysis owing to the long arrival time of blood water in white matter relative to 3 T blood water T_1.

TRUST processing used in-house MATLAB (Mathworks, Natick, MA) scripts. Data were motion-corrected and pairwise subtracted to obtain a difference magnetization image for each of the four effective echo times and four voxels within the sagittal sinus were analysed per subject. Owing to distal venous labelling and identical magnetization transfer effects in control and label conditions, the tissue signals in control and label conditions are identical and can be neglected when analysing the difference signal. The below quantification procedure has been outlined in more detail in the literature (Lu and Ge, 2008). The venous blood water signal in the control scan (S_C^V) can be written:

$$S_C^V = \left(e^{-eTE/T_{2,b}}\right)\left(e^{-TE/T^*_{2,b}}\right) \quad (3)$$

and the venous blood water signal in the label scan (S_L^V) can be written:

$$S_L^V = \left(1 - 2 \cdot e^{-(PLD-eTE)/T_{1,b}}\right)\left(e^{-eTE/T_{2,b}}\right)\left(e^{-TE/T^*_{2,b}}\right) \quad (4)$$

where eTE is the effective echo time, TE is the echo time = 3.6 ms; PLD is the TRUST post-labelling delay time = 1022 ms, $T_{1,b}$ is the 3 T T_1 of blood water, and $T_{2,b}$ and $T^*_{2,b}$ are the transverse and effective transverse relaxation times of blood water in the sagittal sinus voxel, respectively. The difference signal can be written:

$$\Delta S = (S_C^V - S_L^V) = S_0 \cdot e^{eTE \cdot C}$$
$$\text{for } S_0 = 2 \cdot e^{\left(-PLD/T_{1,b} - TE/T^*_{2,b}\right)} \text{ and } C = 1/T_{1,b} - 1/T_{2,b} \quad (5)$$

Therefore, measuring ΔS as a function of eTE allows for determination of S_0, C, and $T_{2,b}$.

$T_{2,b}$ can be related to venous blood oxygenation level (Y_v) when haematocrit is known (Lu *et al.*, 2012). With consideration of the dissolved oxygen in plasma (Xu *et al.*, 2012), the OEF can be written:

$$OEF = \frac{Y_a \cdot C_b + PaO_2 \cdot C_d - Y_v \cdot C_b - PvO_2 \cdot C_d}{Y_a \cdot C_b + PaO_2 \cdot C_d} \quad (6)$$

where Y_a is the arterial oxygen saturation, C_h (8.97 μmol O_2/ml blood) and C_d (0.00138 μmol O_2/ml blood/mmHg O_2 tension) are coefficients associated with the haemoglobin binding ability and plasma-dissolved oxygen. Aside from variations in haematocrit between patients with SCA and control volunteers, C_h is identical for healthy and sickle cell anaemia blood as each haemoglobin molecule has an identical oxygen carrying capacity. As $C_d << C_h$, the influence of plasma-dissolved oxygen is frequently ignored in OEF calculations. However, in SCA the oxygen dissociation curve is shifted, leading to a slightly higher amount of oxygen dissolved in plasma, which will increase the partial pressure of oxygen in blood. Even if the partial pressure of arterial oxygen approaches the alveolar blood oxygen level (e.g. 115 mmHg) this contribution from dissolved oxygen leads to only a small 0.3% increase in OEF. Therefore, in the absence of hyperoxic conditions, the OEF can been simplified to a good approximation to

$$OEF = \frac{Y_a - Y_v}{Y_a} \quad (7)$$

Additional considerations related to the shifting of the oxygen dissociation curve for HbSS are addressed in the 'Discussion' section.

Statistical analysis

First, descriptive statistics, including means, standard deviations, and ranges for continuous parameters were calculated. Investigations for outliers and assumptions for statistical analysis, e.g. normality and homoscedasticity, were made.

The first objective was to assess whether the non-invasive measure of whole-brain OEF was repeatable (e.g. measurement similarity within scan session), reproducible (e.g. measurement similarity between scan sessions), and significantly elevated in the homogenous SCA participants relative to control participants without sickle trait. To assess repeatability and reproducibility, an intraclass correlation coefficient (ICC) was calculated for OEF measurements obtained twice during the same scan session (repeatability) or twice during different scan sessions (reproducibility). To test the difference in OEF, CBF, and normalized tissue volume between controls and patients with SCA, the Wilcoxon rank sum test was applied to determine significant group differences and the Holm method was used to correct for multiple comparisons. A Kruskal-Wallis test was applied to evaluate differences in CBF between flow territories to understand whether any of the CBF trends between patient groups were driven by a specific flow territory.

Finally, to test the secondary hypothesis, volunteers were grouped (e.g. control, SCA with low clinical impairment, or SCA with high clinical impairment) and the Kruskal-Wallis test was used to test for a difference in the means of CBF and OEF measures across groups. In all conditions, corrected $P < 0.05$ was required for significance.

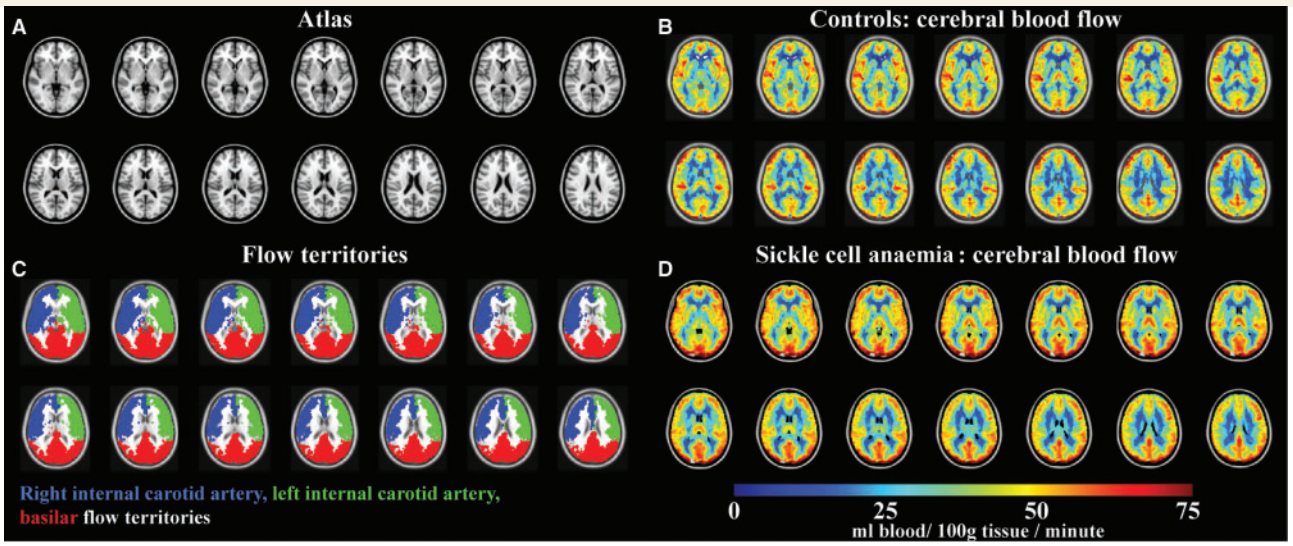

Figure 3 Non-invasive CBF using pseudocontinuous arterial spin labelling imaging in patients with SCA and controls. (**A**) Central slices of a T_1-weighted atlas, along with (**B**) regions analysed for CBF quantification. The flow territories were calculated from vessel-encoded arterial spin labelling data obtained from 92 subjects. CBF maps in (**C**) controls ($n = 11$) and (**D**) participants with SCA ($n = 27$) demonstrate increased CBF in participants with SCA.

Experimental design

Study participants were not randomized or blinded in this observational study.

Results

Table 1 summarizes volunteer demographics. Age and race were matched between controls (age = 26.9 ± 5.1 years) and patients with SCA (age = 27.7 ± 5.0 years) without blood transfusion therapy. All participants were of African-American or Caribbean origin. Blood pressure did not differ between groups, however haematocrit and arterial oxygenation were both reduced ($P < 0.05$) in SCA participants (haematocrit = 27.2 ± 3.6%; arterial oxygen saturation = 95.2 ± 1.8%) relative to control participants (haematocrit = 42.1 ± 5.3%; arterial oxygen saturation = 97.3 ± 1.2%). No control volunteer had a history of prior stroke, silent infarct, or cerebral vasculopathy. Twenty-four of 27 SCA participants were on hydroxyurea (all at appropriate doses > 20 mg per kg per day). Ten of 27 SCA participants had silent infarcts and six had non-specific white matter lesions; two had a history of overt stroke in childhood, though both were small vessel strokes on imaging review and participants were not transfused. All controls had a normal neurological examination with modified Rankin scale scores of zero. Of the 34 adults with sickle cell anaemia, only two had a modified Rankin ⩾ 2. Both participants were in the more impaired group and had a clinical history of overt stroke during childhood. There were an additional five study participants that had mild cognitive issues detectable with a standardized neurological examination, scored as a modified Rankin scale of 1 (no significant disability despite symptoms). One SCA participant on transfusion had moderate intracranial stenosis (51–69%); no SCA participants had cervical stenosis.

The ICC was computed to assess intra-scan reliability of quantitative OEF data. The TRUST measurement was found to have a high repeatability within the same scan session [ICC = 0.989; $P < 0.0001$; 95% CI for ICC = (0.981, 0.994)] and high reproducibility between scans [ICC = 0.952; $P < 0.0001$; 95% CI for ICC = (0.881, 0.986)].

After correcting for haematocrit, $T_{1,b}$ was 1679 ± 86 ms in control participants and 1936 ± 77 ms in SCA participants. The longer $T_{1,b}$ in SCA participants will lead to an overestimation of CBF in anaemic participants if not taken into account. Figure 3 shows the results of the CBF data, depicting clear increased CBF in all major flow territories (two-tailed $P < 0.001$). Mean CBF within cortical grey matter regions (all territories in Fig. 3B) in control participants was 43.6 ± 5.1 ml/100 g/min [interquartile range (IQR) = 40.4–45.9 ml/100 g/min) and 51.0 ± 6.5 ml/100 g/min (IQR = 46.2–56.8 ml/100 g/min) in SCA participants (Table 1). There was no significant difference in CBF between flow territories for either the control participants or SCA participants.

Figure 4 shows graphical representations of the imaging findings as boxplots with data points overlaid. The central black line on the box plot depicts the median of the data, top and bottom solid lines depict 25th and 75th percentile of the data, and whiskers extend to all data points not determined to be outliers. After adjusting for multiple comparisons, an increase in tissue volume normalized by intracranial volume was observed in controls versus SCA participants ($P = 0.015$), which was also observed when

Table 1 Summary of study participants with and without SCA

Variables	Control participants ($n = 11$)	SCA participants ($n = 27$)
Age (years)	26.9 ± 5.1	27.7 ± 5.0
Sex (% male)	45	59
Race (% African-American)	100	100
Systolic blood pressure (mmHg)	111 ± 12	118 ± 15
Diastolic blood pressure (mmHg)	67 ± 13	69 ± 12
Haematocrit (%)	42.1 ± 5.3	27.2 ± 3.6
Haemoglobin S (%)	0	64.8 ± 20.6
Arterial oxygen saturation(%; measured by pulse oximetry)	97.3 ± 1.2	95.2 ± 1.8
Venous oxygen saturation(%; measured from TRUST)	63.2 ± 6.1	52.0 ± 7.5
OEF (%)	35.0 ± 6.1	45.3 ± 7.5
CBF (ml blood/100 g tissue/ minute)	44.1 ± 5.2	51.0 ± 6.5
Venous blood water T_2 (ms)	66.2 ± 11.3	77.5 ± 10.4
Grey matter volume / intracranial volume	0.388 ± 0.017	0.388 ± 0.026
White matter volume / intracranial volume	0.413 ± 0.018	0.395 ± 0.022
CSF volume / intracranial volume	0.199 ± 0.013	0.216 ± 0.018

SCA participants are those used for testing the primary hypothesis of the study and are not on blood transfusion. All values are mean ± SD. Grey matter volume and white matter volume units are mm^3 but when normalized for intracranial volume, the ratio is dimensionless.

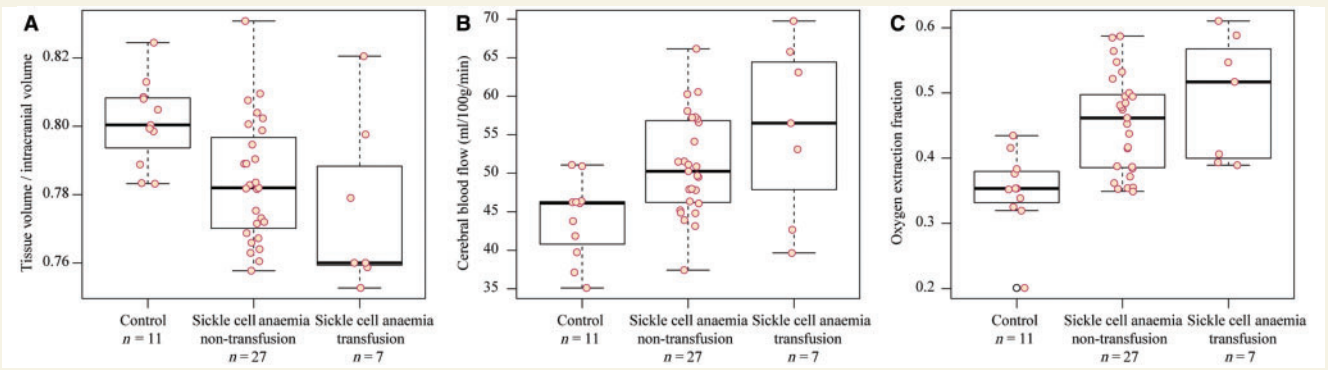

Figure 4 Volumetric, CBF, and OEF analysis in SCA participants and control volunteers. Controls ($n = 11$), SCA participants not on blood transfusion and without a history of prior overt stroke ($n = 27$) and SCA participants on blood transfusion ($n = 7$) are shown, however to reduce confounds from patient heterogeneity only non-transfusion patients were used for testing the primary hypothesis of the study. Tissue volumes (**A**) are significantly reduced in non-transfusion patients versus control volunteers. CBF (**B**) is elevated ($P < 0.05$) in the cortical mask (Fig. 3) of non-transfusion patient versus controls and did not differ significantly between flow territories. OEF (**C**) is also elevated ($P < 0.05$) in non-transfusion patients relative to controls. The central black line on the box plot depicts the median of the data, top and bottom solid lines depict 25th and 75th percentile of the data, and whiskers extend to all data points not determined to be outliers. Actual data points are overlaid on boxplots as red circles (black circles for outliers).

controls versus SCA participants on blood transfusion were considered (adjusted $P = 0.047$). Control volunteers had reduced CBF compared to non-transfusion SCA participants (adjusted $P = 0.0149$) but not transfusion SCA participants (adjusted $P = 0.0882$). Consistent with the primary hypothesis of the study, the control group had a significantly lower OEF compared with the non-transfusion SCA participants, pairwise comparisons using the Wilcoxon rank sum test (adjusted $P = 0.0012$) and transfusion SCA participants (adjusted $P = 0.0075$).

The secondary hypothesis of the study was that in SCA participants meeting criteria for higher levels of clinical impairment, OEF is highest. We found a significant increase (Fig. 5A) in OEF in more impaired SCA volunteers (OEF = 0.489 ± 0.074) versus less impaired SCA (OEF = 0.426 ± 0.075) and healthy control volunteers (0.350 ± 0.061) (Kruskal-Wallis test, $P < 0.0001$). The CBF difference (Fig. 5B) was less significant with SCA participants with higher impairment having more varied CBF ($P = 0.015$). These findings provided evidence in favour of the secondary hypothesis of the study, and suggest that elevated OEF may be a more specific indicator of impairment than elevated CBF in adults with sickle cell anaemia.

Figure 6 shows an example of images from a representative control volunteer (Fig. 6A) and two SCA participants (Fig. 6B and C).

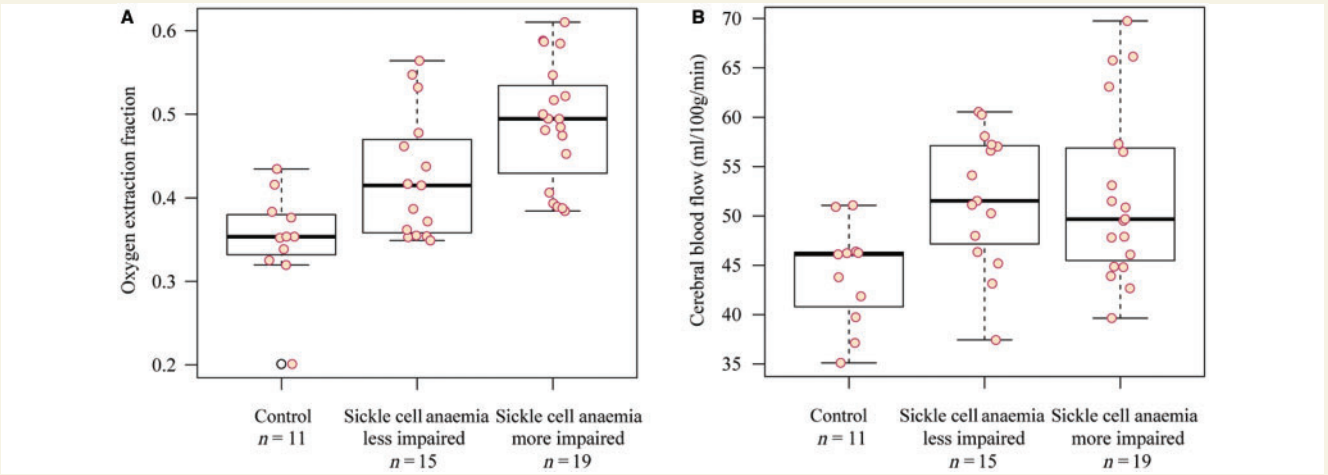

Figure 5 Results of the secondary study aim, which was to assess how OEF and CBF varied for SCA participants with less or more impairment as defined by clinical criteria. OEF (**A**) was elevated in more impaired patients ($P < 0.001$), whereas CBF (**B**) was not different ($P = 0.088$) between SCA groups with different levels of impairment, likely due to multiple competing effects related to reduced oxygen carrying capacity and steno-occlusion.

Discussion

We have demonstrated the ability to apply TRUST MRI to measure whole-brain OEF-weighted contrast quickly (e.g. < 2 min) in adults with SCA. Results show significant elevations in quantified OEF in young adults with SCA compared to healthy controls and evidence is provided for OEF increasing with increasing levels of clinical impairment. Acquisition takes only 1–2 min and calculations required to quantify OEF take ~1 min and require only a routine haematocrit and measurement of arterial oxygen saturation via pulse oximetry.

Interpretation of haemo-metabolic findings

While not definitively established, elevated OEF in participants with SCA compared to healthy controls is reasonable based on prior literature in adults with intracranial stenosis (Derdeyn *et al.*, 1999, 2001) and anaemia (Dhar *et al.*, 2009).

In patients with SCA, oxygen carrying capacity (C_a), which depends on the arterial oxygen saturation and haematocrit, is reduced; this may be compensated for by an increase in CBF through autoregulation. If CBF cannot increase sufficiently to compensate for the reduced oxygen carrying capacity, the OEF will begin to increase for constant $CMRO_2$:

$$OEF = \frac{oxygen\ consumed}{oxygen\ delivered} = \frac{CMRO_2}{CBF \cdot C_a} \quad (8)$$

As such, it is possible that CBF increases may outweigh increases in OEF, especially in early stages of impairment. For instance, the SCA participant shown in Fig. 6B with prior small ischaemic strokes has a lower OEF than the participant in Fig. 6C, but also much higher CBF. It is possible that this participant is better able to compensate for reduced oxygen carrying capacity by increasing CBF. Partly owing to practical difficulties of measuring OEF using invasive procedures, this hypothesis has not yet been rigorously evaluated in a large cohort of sickle cell anaemia patients. However, the non-invasive nature of the TRUST protocol, performed in sequence with non-invasive pCASL (pseudo-continuous arterial spin labeling) may allow for this possibility to be studied, along with the relationships between elevated OEF, hyperaemia, and stroke risk.

We observed a relatively large variation in OEF among SCA participants, similar to that in a $_{15}O$ PET study of OEF (Herold *et al.*, 1986), and as such this measure may provide discriminatory value for assessing future stroke risk. While both CBF and OEF were found to be elevated in patients with SCA relative to control volunteers, there is also a large range of variability in both CBF and OEF measures (Fig. 4), which motivates the relevance of contrasting OEF with CBF for discriminating stroke risk in patients with SCA (Fig. 1).

Considering how the OEF and CBF values relate to the proposed physiological model (Fig. 1) is also useful. In a supplementary analysis (Supplementary Fig. 1), we evaluated the relationship between OEF and CBF in participants, and as expected an inverse correlation was present across all patients ($P = 0.04$), but this correlation was strongest in the less impaired patients ($P = 0.02$) and not significant for the more impaired patients ($P = 0.17$), which is consistent with OEF and CBF providing discrepant information in more advanced stages of disease. We also combined OEF and CBF to estimate $CMRO_2$ using an identical procedure as has been outlined previously (Xu *et al.*, 2009) and we observed no difference ($P = 0.10$) in $CMRO_2$ between

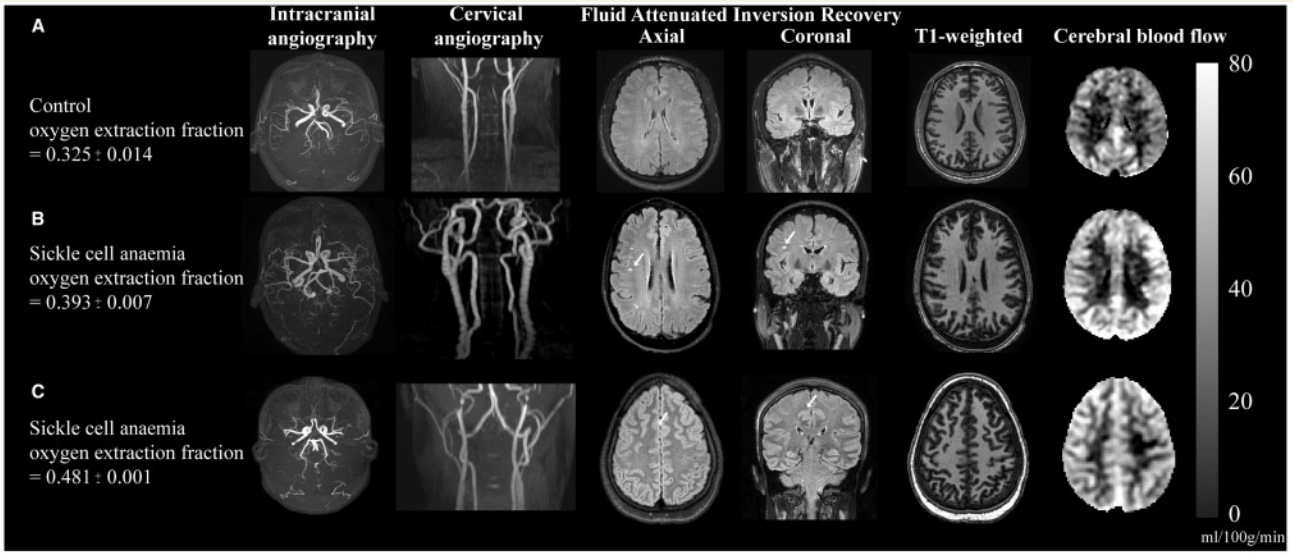

Figure 6 Individual case examples of structural and haemo-metabolic imaging. (**A**) Control: A healthy 25-year-old male control with no vasculopathy or prior infarcts. Mean CBF in the grey matter mask (Fig. 3) is 40.6 ml/100 g/min and whole-brain OEF is 0.325, consistent with normal values. (**B**) Adult with SCA and silent strokes: A 29-year-old male with SCA on regular blood transfusion therapy for recurrent pain crises. His baseline haemoglobin is 7.7 g/dl, and his pulse oximetry shows an oxygen saturation of 95%. Magnetic resonance angiography of the brain does not reveal any vasculopathy, but prior silent strokes without overt neurological symptoms are apparent on FLAIR imaging (white arrows). The CBF is elevated relative to the control at 60.5 ml/100 g/min, as is the OEF = 0.393. (**C**) Adult with SCA and progressive infarcts: 25-year-old female with SCA with no history of overt stroke but silent cerebral infarcts apparent on MRI and elevated OEF on her study MRI with recurrent infarcts after this MRI. Her baseline haemoglobin was 7.7 g/dl, and pulse oximetry oxygen saturation of 92.5%. MRI shows a silent cerebral infarct (white arrow, axial and coronal views). Normal magnetic resonance angiography head and neck but CBF and OEF were elevated relative to controls at 51.3 ml/100 g/min and 0.48, respectively. Approximately 1 week after this study MRI, she presented with a typical pain crisis and developed a persistent headache. Clinical MRI showed two punctate foci of restricted diffusion consistent with new, tiny infarcts. Colour bar on *right* denotes CBF in units of ml/100 g/min.

patients and controls and only a very weak and non-significant trend between haematocrit and CBF in patients, indicative of additional complex mechanisms underlying sources of CBF discrepancy between patients (which could include HbS fraction, CBV, or vasculopathy extent). Additional data over a wider range of impairment are required to rigorously evaluate and refine the model.

SCA confers an increased risk of stroke, 3 to 10-fold in adults (Strouse *et al.*, 2011) and 100-fold in children (Earley *et al.*, 1998) compared to age, race and gender-matched populations without SCA. In children aged 2–16 years with SCA, standard care for primary prevention of strokes includes transcranial Doppler ultrasound measurements and for those with elevated measurements, institution of monthly blood transfusion therapy (Balkaran *et al.*, 1992; Pegelow *et al.*, 2002). This therapy has resulted in a log-fold decrease in the rate of overt strokes in children. However, no accepted technology exists that identifies adults with SCA who will have a first or recurrent stroke as transcranial Doppler ultrasound assessment has not been proven to be beneficial to individuals older than 16 to lack of validation and in 6% due to technical limitations related to skull thickness (Valadi *et al.*, 2006; Silva *et al.*, 2009). Moreover, some children on regular blood transfusion therapy for secondary stroke prevention have their transfusions discontinued in early adulthood due to patient preference, burden of life-long transfusion therapy and inability to estimate future stroke risk. Therefore, there is an urgent need for improved screening procedures for adults with SCA that may be used to predict stroke risk. Elevated OEF may serve as an imaging biomarker for stratifying patients with tenuous cerebrovascular reserves who may stand to benefit most from aggressive stroke prevention strategies.

Oxygen extraction fraction measurement approaches

In this study, we used a relatively novel, non-invasive MRI approach that provides information on whole-brain OEF. While $_{15}$O PET is considered the gold-standard for OEF imaging, PET requires $_{15}$O which has a short half-life of 2–3 min, an arterial line, and exposure to ionizing radiation. While this method has greatly expanded our understanding of cerebral physiology, it is suboptimal as a routine screening tool in non-specialized centres, or for evaluating short-term treatment responses. For these

reasons we evaluated a non-invasive method. Our protocol used a fast scan time of 1–2 min without the requirement of extensive user planning or expertise, and therefore may be applicable in clinical protocols where time-consuming planning is not practical. Finally, newer imaging methods are being proposed that enable more regional assessment of blood oxygenation using similar principles of spin labelling and T_2 mapping (Bolar *et al.*, 2011; Guo and Wong, 2012; Krishnamurthy *et al.*, 2014; An *et al.*, 2015), additional T_1 quantification (De Vis *et al.*, 2014), or susceptibility-weighting (Driver *et al.*, 2014). These methods may be especially applicable as an extension of the method used here in patients with regional elevations in OEF secondary to focal ischaemia.

Limitations

The findings of this work should also be considered in the context of several limitations. First, our sample size of 34 SCA participants and 11 controls was modest, which limits the extent of clinical interpretation. However, our sample size was matched for age, race, and vasculopathy extent. Second, we recruited a fairly healthy population of adults with SCA as none of the 27 participants in the primary analysis had major large vessel stroke or moderate or severe cerebral vasculopathy. A next step will be to assess this technique in SCA participants with significant intracranial stenosis. Third, arterial oxygen saturations utilized to calculate OEF were measured by pulse oximetry rather than by the gold standard arterial blood sampling. Pulse oximetry is known to have reduced accuracy in SCA and may underestimate arterial oxygen saturations (Rackoff *et al.*, 1993). We simulated this bias and found that a systematic bias of $\sim$15% would be required to account for our OEF differences between SCA participants and controls, yet studies have reported a smaller 1.1% difference (Ortiz *et al.*, 1999). Therefore, while our pulse oximetry estimated arterial oxygenation values in participants with SCA may be slightly inaccurate, they likely cannot account for the inter-group findings. Fourth, the pCASL labelling efficiency will depend on the velocity of blood through the labelling plane, which may differ between SCA versus controls. We applied quantitative velocity phase contrast angiography in a subgroup of our patients ($n = 24$) and controls ($n = 7$) and observed a modest increase in internal carotid artery velocity of $\sim$19%, which would lead to a reduction in pCASL labelling efficiency, thereby slightly underestimating the CBF in patients. As such, the true CBF in SCA may be even higher than what is reported here. Cervical blood velocity, cardiac output, and stenosis degree to our knowledge have never been included in individualized pCASL labelling efficiencies; however this may be an important topic for future work. Fifth, the calibration models applied here are based on blood with HbAA, yet may require modification for blood with HbSS. To ensure that blood water T_1 and T_2 were not overwhelmingly different for similar haematocrit and oxygenation level in blood with HbAA versus HbSS, we performed *ex vivo* measurements (Supplementary Fig. 2). Only small variations in T_1 and T_2 were observed between these blood samples, which could not account for the findings reported here. However, more work over a wider range of oxygenation and haematocrit values is certainly warranted. Finally, we chose to focus on a relatively homogenous sample of adults with SCA and to not include those receiving blood transfusion in the primary analysis. Further studies in a larger volume of patients will allow for the influence of treatment effects on OEF and CBF to be evaluated.

Conclusion

We present the first application of non-invasive TRUST MRI in adults with SCA and have demonstrated abilities to detect elevated OEF in SCA participants, relative to control volunteers, done quickly and without exogenous contrast agents. These data justify larger clinical studies aimed at understanding the relationships between metabolism, perfusion, stroke risk, and therapy response in adults with SCA for whom stroke screening procedures are unavailable.

Acknowledgements

We are grateful to Carlos Faraco, Christopher Thompson, Claire Kurtenbach, Chaohui Tang, Kristen George-Durrett, and Leslie McIntosh for experimental support.

Funding

Funding provided by the American Heart Association (14CSA20380466), NIH/NINDS (5R01NS078828).

Supplementary material

Supplementary material is available at *Brain* online.

References

Adams RJ, McKie VC, Brambilla D, Carl E, Gallagher D, Nichols FT, et al. Stroke prevention trial in sickle cell anemia. Control Clin Trials 1998a; 19: 110–29.

Adams RJ, McKie VC, Hsu L, Files B, Vichinsky E, Pegelow C, et al. Prevention of a first stroke by transfusions in children with sickle cell anemia and abnormal results on transcranial Doppler ultrasonography. N Engl J Med 1998b; 339: 5–11.

Alsop DC, Detre JA, Golay X, Gunther M, Hendrikse J, Hernandez-Garcia L, et al. Recommended implementation of arterial spin-labeled perfusion MRI for clinical applications: A consensus of the ISMRM perfusion study group and the European consortium for ASL in dementia. Magn Reson Med 2015; 73: 102–16.

An H, Ford AL, Chen Y, Zhu H, Ponisio R, Kumar G, et al. Defining the ischemic penumbra using magnetic resonance oxygen metabolic index. Stroke 2015; 46: 982–8.

Balkaran B, Char G, Morris JS, Thomas PW, Serjeant BE, Serjeant GR. Stroke in a cohort of patients with homozygous sickle cell disease. J Pediatr 1992; 120: 360–6.

Banks JL, Marotta CA. Outcomes validity and reliability of the modified Rankin scale: implications for stroke clinical trials: a literature review and synthesis. Stroke 2007; 38: 1091–6.

Bolar DS, Rosen BR, Sorensen AG, Adalsteinsson E. Quantitative imaging of eXtraction of oxygen and TIssue consumption (QUIXOTIC) using venular-targeted velocity-selective spin labeling. Magn Reson Med 2011; 66: 1550–62.

Casella JF, King AA, Barton B, White DA, Noetzel MJ, Ichord RN, et al. Design of the silent cerebral infarct transfusion (SIT) trial. Pediatr Hematol Oncol 2010; 27: 69–89.

De Vis JB, Petersen ET, Alderliesten T, Groenendaal F, de Vries LS, van Bel F, et al. Non-invasive MRI measurements of venous oxygenation, oxygen extraction fraction and oxygen consumption in neonates. NeuroImage 2014; 95: 185–92.

Debaun MR, Derdeyn CP, McKinstry RC III. Etiology of strokes in children with sickle cell anemia. Ment Retard Dev Disabil Res Rev 2006; 12: 192–9.

Derdeyn CP, Grubb RL Jr, Powers WJ. Cerebral hemodynamic impairment: methods of measurement and association with stroke risk. Neurology 1999; 53: 251–9.

Derdeyn CP, Videen TO, Grubb RL Jr, Powers WJ. Comparison of PET oxygen extraction fraction methods for the prediction of stroke risk. J Nucl Med 2001; 42: 1195–7.

Derdeyn CP, Videen TO, Yundt KD, Fritsch SM, Carpenter DA, Grubb RL, et al. Variability of cerebral blood volume and oxygen extraction: stages of cerebral haemodynamic impairment revisited. Brain 2002; 125 (Pt 3): 595–607.

Dhar R, Zazulia AR, Videen TO, Zipfel GJ, Derdeyn CP, Diringer MN. Red blood cell transfusion increases cerebral oxygen delivery in anemic patients with subarachnoid hemorrhage. Stroke 2009; 40: 3039–44.

Donahue MJ, Faraco CC, Strother MK, Chappell MA, Rane S, Dethrage LM, et al. Bolus arrival time and cerebral blood flow responses to hypercarbia. J Cereb Blood Flow Metab 2014; 34: 1243–52.

Driver ID, Wharton SJ, Croal PL, Bowtell R, Francis ST, Gowland PA. Global intravascular and local hyperoxia contrast phase-based blood oxygenation measurements. NeuroImage 2014; 101: 458–65.

Earley CJ, Kittner SJ, Feeser BR, Gardner J, Epstein A, Wozniak MA, et al. Stroke in children and sickle-cell disease: Baltimore-Washington cooperative young stroke study. Neurology 1998; 51: 169–76.

Faraco CC, Strother MK, Dethrage LM, Jordan L, Singer R, Clemmons PF, et al. Dual echo vessel-encoded ASL for simultaneous BOLD and CBF reactivity assessment in patients with ischemic cerebrovascular disease. Magn Reson Med 2015; 73: 1579–92.

Fox PT, Raichle ME. Focal physiological uncoupling of cerebral blood flow and oxidative metabolism during somatosensory stimulation in human subjects. Proc Natl Acad Sci USA 1986; 83: 1140–4.

Ge Y, Zhang Z, Lu H, Tang L, Jaggi H, Herbert J, et al. Characterizing brain oxygen metabolism in patients with multiple sclerosis with T2-relaxation-under-spin-tagging MRI. J Cereb blood Flow Metab 2012; 32: 403–12.

Guo J, Wong EC. Venous oxygenation mapping using velocity-selective excitation and arterial nulling. Magn Reson Med 2012; 68: 1458–71.

Herold S, Brozovic M, Gibbs J, Lammertsma AA, Leenders KL, Carr D, et al. Measurement of regional cerebral blood flow, blood volume and oxygen metabolism in patients with sickle cell disease using positron emission tomography. Stroke 1986; 17: 692–8.

Hudak ML, Jones MD Jr, Popel AS, Koehler RC, Traystman RJ, Zeger SL. Hemodilution causes size-dependent constriction of pial arterioles in the cat. Am J Physiol 1989; 257 (3 Pt 2): H912–17.

Hulbert ML, Ford AL. Understanding sickle cell brain drain. Blood 2014; 124: 830–1.

Hulbert ML, McKinstry RC, Lacey JL, Moran CJ, Panepinto JA, Thompson AA, et al. Silent cerebral infarcts occur despite regular blood transfusion therapy after first strokes in children with sickle cell disease. Blood 2011; 117: 772–9.

Jenkinson M, Smith S. A global optimisation method for robust affine registration of brain images. Med Image Anal 2001; 5: 143–56.

Krishnamurthy LC, Liu P, Xu F, Uh J, Dimitrov I, Lu H. Dependence of blood T(2) on oxygenation at 7 T: in vitro calibration and in vivo application. Magn Reson Med 2014; 71: 2035–42.

Liu P, Huang H, Rollins N, Chalak LF, Jeon T, Halovanic C, et al. Quantitative assessment of global cerebral metabolic rate of oxygen (CMRO2) in neonates using MRI. NMR Biomed 2014; 27: 332–40.

Lu H, Clingman C, Golay X, van Zijl PC. Determining the longitudinal relaxation time (T1) of blood at 3.0 Tesla. Magn Reson Med 2004; 52: 679–82.

Lu H, Donahue MJ, van Zijl PC. Detrimental effects of BOLD signal in arterial spin labeling fMRI at high field strength. Magn Reson Med 2006; 56: 546–52.

Lu H, Ge Y. Quantitative evaluation of oxygenation in venous vessels using T2-Relaxation-Under-Spin-Tagging MRI. Magn Reson Med 2008; 60: 357–63.

Lu H, Xu F, Grgac K, Liu P, Qin Q, van Zijl P. Calibration and validation of TRUST MRI for the estimation of cerebral blood oxygenation. Magn Reson Med 2012; 67: 42–9.

Lu H, Xu F, Rodrigue KM, Kennedy KM, Cheng Y, Flicker B, et al. Alterations in cerebral metabolic rate and blood supply across the adult lifespan. Cereb Cortex 2011; 21: 1426–34.

National Heart Lung and Blood Institute (NHLBI). NIH ends Transcranial Doppler (TCD) with Transfusions Changing to Hydroxyurea (TWiTCH) clinical trial due to early results. 2014. Available from: http://www.nih.gov/news/health/nov2014/nhlbi-19.htm (1 April 2015, date last accessed).

Ohene-Frempong K, Weiner SJ, Sleeper LA, Miller ST, Embury S, Moohr JW, et al. Cerebrovascular accidents in sickle cell disease: rates and risk factors. Blood 1998; 91: 288–94.

Ortiz FO, Aldrich TK, Nagel RL, Benjamin LJ. Accuracy of pulse oximetry in sickle cell disease. Am J Respir Crit Care Med 1999; 159: 447–51.

Pegelow CH, Macklin EA, Moser FG, Wang WC, Bello JA, Miller ST, et al. Longitudinal changes in brain magnetic resonance imaging findings in children with sickle cell disease. Blood 2002; 99: 3014–18.

Powers WJ. Cerebral hemodynamics in ischemic cerebrovascular disease. Ann Neurol 1991; 29: 231–40.

Prohovnik I, Hurlet-Jensen A, Adams R, De Vivo D, Pavlakis SG. Hemodynamic etiology of elevated flow velocity and stroke in sickle-cell disease. J Cereb Blood Flow Metab 2009; 29: 803–10.

Rackoff WR, Kunkel N, Silber JH, Asakura T, Ohene-Frempong K. Pulse oximetry and factors associated with hemoglobin oxygen desaturation in children with sickle cell disease. Blood 1993; 81: 3422–7.

Rane S, Ally B, Mason E, Pradhan S, Hussey E, Waddell KW, et al. Relationships between excitation-inhibition balance and whole-brain oxygen extraction fraction in human brain. In: ISMRM 23rd Annual Meeting & Exhibition 2015, Toronto, ON, Canada, 2015.

Silva GS, Vicari P, Figueiredo MS, Carrete H Jr, Idagawa MH, Massaro AR. Brain magnetic resonance imaging abnormalities in adult patients with sickle cell disease: correlation with transcranial Doppler findings. Stroke 2009; 40: 2408–12.

Strouse JJ, Lanzkron S, Urrutia V. The epidemiology, evaluation and treatment of stroke in adults with sickle cell disease. Expert Rev Hematol 2011; 4: 597–606.

Valadi N, Silva GS, Bowman LS, Ramsingh D, Vicari P, Filho AC, et al. Transcranial Doppler ultrasonography in adults with sickle cell disease. Neurology 2006; 67: 572–4.

Vorstrup S, Lass P, Waldemar G, Brandi L, Schmidt JF, Johnsen A, et al. Increased cerebral blood flow in anemic patients on long-term hemodialytic treatment. J Cerebral Blood Flow Metab 1992; 12: 745–9.

Wardlaw JM, Smith EE, Biessels GJ, Cordonnier C, Fazekas F, Frayne R, et al. Neuroimaging standards for research into small vessel disease and its contribution to ageing and neurodegeneration. Lancet Neurol 2013; 12: 822–38.

Xu F, Ge Y, Lu H. Noninvasive quantification of whole-brain cerebral metabolic rate of oxygen (CMRO2) by MRI. Magn Reson Med 2009; 62: 141–8.

Xu F, Liu P, Pascual JM, Xiao G, Lu H. Effect of hypoxia and hyperoxia on cerebral blood flow, blood oxygenation, and oxidative metabolism. J Cereb Blood Flow Metab 2012; 32: 1909–18.

Zhang Y, Brady M, Smith S. Segmentation of brain MR images through a hidden Markov random field model and the expectation-maximization algorithm. IEEE Trans Med Imaging 2001; 20: 45–57.

Zhao JM, Clingman CS, Narvainen MJ, Kauppinen RA, van Zijl PC. Oxygenation and hematocrit dependence of transverse relaxation rates of blood at 3T. Magn Reson Med 2007; 58: 592–7.